This article has been accepted for publication in 2018 International Symposium on Wearable Robotics and Rehabilitation (WeRob 2018).
Citation information including DOI would be available once published on IEEE Xplore Digital Library.

Design of a Hand Exoskeleton for Use with Upper Limb Exoskeletons

Peter Walker Ferguson*, Brando Dimapasoc*, Yang Shen, and Jacob Rosen

***Abstract*— Due to high degree of freedom and different mechanism foci, hand and arm exoskeletons are usually developed separately and seldom combined together. Hand exoskeletons are typically more complex mechanisms than arm or leg exoskeletons due to the numerous degrees of freedom encapsulated in the hand and the small anatomical structure involved. This study presents the design of a 12 DOF (6 active) reconfigurable hand exoskeleton for rehabilitation that will be installed on the existing upper limb exoskeleton, EXO-UL8. Given the mechanism architecture, a nonlinear optimization framework minimizes physical footprint while maximizing mechanism isotropy and device functionality.**

I. INTRODUCTION

For decades, stroke has been one of the leading diseases that causes long-term disabilities [1]. Researchers and physical therapists have been working on exoskeleton-like robots to help patients regain capabilities post stroke. The upper limb is an area of focus, but research has focused mainly on individual parts, either arm or hand [2][3][4]. Although there is a need for rehabilitating the capabilities in reach and grasp activities of daily living (ADLs), only a handful of systems have a working combination of both arm and hand [5][6]. Even fewer combination systems actively actuate multiple DOFs across multiple fingers [7]. Based on our existing upper limb exoskeleton system, EXO-UL8 [8], a reconfigurable hand exoskeleton is designed.

II. METHODS

A. Design Requirements:

The following requirements were formulated for a rehabilitation hand exoskeleton that attaches to an arm exoskeleton:

1) Low Mass: Mass at the hand must be minimized to reduce required torque of the upper limb exoskeleton.
2) Torque: The torque capabilities of the exoskeleton must be sufficiently large to actuate the hand.
3) Workspace: The workspace of the exoskeleton must contain the workspace of the human hand.
4) Grasp: It must be able to actuate a variety of grasps.
5) Open Palm: It must leave the palm and fingers unoccupied to permit interaction with physical objects.
6) Unisize: It must fit 95% of the general population.

This work was funded in part by the National Science Foundation through Award #1532239.

*These authors contributed equally to this work.

P. W. Ferguson, B. Dimapasoc, Y. Shen, and J. Rosen are with the Bionics Laboratory at the University of California Los Angeles, Los Angeles, CA 90095 USA (e-mail: PWFerguson@ucla.edu).

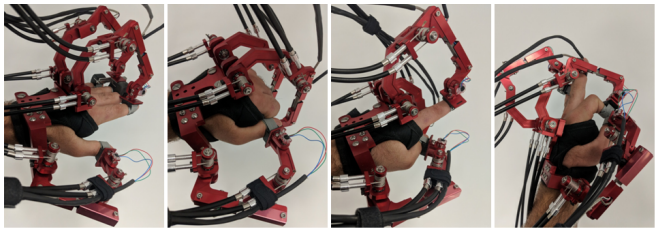

Fig. 1. 1-1-3 Configuration shown with (A): Open Hand, (B): Closed Fist, (C): Pointing, (D): Pincer Grasp.

B. Actuation Method:

For the low mass and torque requirements, a Bowden cable transmission system with brushed DC motors was chosen. The cable transmission enabled remote location of the motor pack, reducing mass at the hand. It also allowed use of oversized actuators with sufficient torque for hand rehabilitation.

C. Basic Topology:

Workspace, grasp, open palm, and unisize requirements were satisfied with a reconfigurable design topology of three 3R planar serial linkages that attach on the dorsal side of the hand to the distal phalanges. Three linkages are used because 95% of human grasps are achievable with a thumb and two fingers [9]. The topology does not impede grasping physical objects and allows a one-size-fits-all design that does not require adjustment for different finger lengths. The third joint was made passive in order to decrease complexity and inertia compared to an active joint. Due to the link lengths, this joint mainly relates to orientation as opposed to position. The addition of a passive rotational joint at the end-effector of both finger linkages permits adduction/abduction over small ranges to improve comfort and allow more natural movement. Bending beam load cells were used as the structure of the first link (L_1) of the thumb linkage and second link (L_2) of the finger linkages to enable admittance control.

The linkages are reconfigurable to enable a variety of grasps. The first linkage attaches from above the carpometacarpal (CPC) joint to the distal phalanx of the thumb. The plane of the workspace of this linkage is adjustable via rotation around the CPC. The second and third linkages connect from above the metacarpophalangeal (MCP) joints to the distal phalanges of the fingers. The origin of these linkages is adjustable for different hand widths or to place them in plane with different fingers. The distal end of the second and third linkage feature interchangeable customizable 3D-printed finger attachments that enable different sets of fingers to be actuated by each linkage. Notable configurations

include 1-1-3 (thumb, index, middle+ring+little) and 1-2-2 (thumb, index+middle, ring+little). The 1-1-3 configuration is shown for a set of representative hand positions in Fig. 1. To account for motion of the little finger relative to the ring finger, a passive slider mechanism connects the finger attachment for the little finger to the third linkage.

D. Link Length Optimization:

To satisfy the unisize requirement, the link lengths were chosen via a brute force optimization algorithm considering fingers in the 95th percentile for length.

The lengths of L_1 of the thumb linkage and L_2 of the finger linkages were set to 8.9cm due to the length of the bending beam load cells. For each linkage, the remaining link lengths were varied across a reasonable range. Each combination, L, of potential link lengths L_1, L_2, and L_3, was checked for kinematic feasibility. Forward and inverse kinematics were used to verify that the linkage could correctly attach to the tip of the distal phalanx of the appropriate finger at all combinations of joint angles (θ_1,θ_2,θ_3) within the workspace with 3° resolution. To correctly attach, L_3 must be capable of connecting perpendicularly to the dorsal side of the distal phalanx, and the joints of the linkage must not physically touch or cross through the finger.

A design score, J, was calculated for each L based on mechanism isotropy and link length. Mechanism isotropy (ISO), a function of the joint angles is a measure of kinematic performance. It is defined in 1 as the ratio of the min (λ_{min}) and max (λ_{max}) eigenvalue of the Jacobian matrix.

$$ISO(\theta_1, \theta_2, \theta_3) = \frac{\lambda_{min}}{\lambda_{max}} \in (0, 1) \tag{1}$$

An isotropy value of 0 indicates a singularity and a loss of a degree of freedom, while a value of 1 indicates that the end effector can move equally well in all directions.

Mechanism isotropy is calculated for each set of joint angles previously mentioned. To account for varying densities of the end effector location in these sets, the finger workspace area is discretized into a grid of cells, K, and the isotropy is averaged for each cell. Summing the average isotropy of the cells provides an indication of the kinematic capabilities of the mechanism across the entire workspace. It is desirable for the mechanism to avoid singular or near-singular configuration within the workspace of the finger. Therefore, J of each L is proportional to both overall performance (sum of ISO) and to worst-case performance (minimum ISO value calculated).

As mechanical isotropy tends to reward longer link lengths, but it is desirable to keep size and mass of the mechanism low, an additional term is included in J score to reward shorter designs. This was accomplished by making J inversely proportional to the sum of the link lengths raised to a hyperparameter A, as shown in 2. A prototype with adjustable link lengths was used to experimentally verify the design produced by a variety of A. Based on this verification, link lengths were chosen for each linkage.

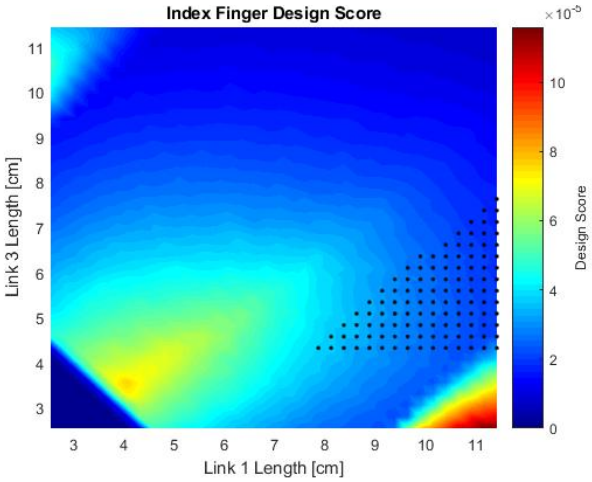

Fig. 2. Optimization results for the linkage connecting to the index finger for A=5. Dots represent kinematically valid combinations of L_1 and L_3 for L_2=8.9cm. Set $L_1 \geq$ 4.4cm due to minimum axes size.

$$J = \frac{\Sigma_K ISO(\theta_1, \theta_2, \theta_3) * MIN_K(ISO(\theta_1, \theta_2, \theta_3))}{(L_1 + L_2 + L_3)^A} \tag{2}$$

The results of the optimization are illustrated for the linkage that connects to the index finger in Fig. 2.

III. Conclusion

The hand exoskeleton presented is multi-fingered, multi-DOF, physically reconfigurable, and designed to attach to a full-arm exoskeleton. The link lengths were determined by optimization for maximized mechanism isotropy and minimized footprint.

References

[1] E. J. Benjamin *et al.*, "Heart disease and stroke statistics—2017 update: A report from the american heart association," *Circulation*, 2017.

[2] A. Wege and A. Zimmermann, "Electromyography sensor based control for a hand exoskeleton," in *2007 IEEE Int. Conf. on Robotics and Biomimetics (ROBIO)*, Dec 2007, pp. 1470–1475.

[3] N. S. K. Ho *et al.*, "An emg-driven exoskeleton hand robotic training device on chronic stroke subjects: Task training system for stroke rehabilitation," in *2011 IEEE Int. Conf. on Rehabilitation Robotics*, June 2011, pp. 1–5.

[4] C. N. Schabowsky, S. B. Godfrey, R. J. Holley, and P. S. Lum, "Development and pilot testing of hexorr: Hand exoskeleton rehabilitation robot," *Journal of NeuroEngineering and Rehabilitation*, vol. 7, no. 1, p. 36, Jul 2010.

[5] Y. Ren, H. S. Park, and L. Q. Zhang, "Developing a whole-arm exoskeleton robot with hand opening and closing mechanism for upper limb stroke rehabilitation," in *2009 IEEE Int. Conf. on Rehabilitation Robotics*, June 2009, pp. 761–765.

[6] A. Frisoli *et al.*, "A new force-feedback arm exoskeleton for haptic interaction in virtual environments," in *First Joint Eurohaptics Conf. and Symp. on Haptic Interfaces for Virtual Environment and Teleoperator Systems. World Haptics Conf.*, March 2005, pp. 195–201.

[7] C. Lauretti *et al.*, "Learning by demonstration for motion planning of upper-limb exoskeletons," *Frontiers in Neurorobotics*, vol. 12, p. 5, 2018.

[8] Y. Shen, J. Ma, B. Dobkin, and J. Rosen, "Asymmetric dual arm approach for post stroke recovery of motor function utilizing the exo-ul8 exoskeleton system: A pilot study," in *Engineering in Medicine and Biology Society (EMBC)*, June 2018.

[9] I. Kapandji, L. Honoré, and F. Poilleux, *Upper Limb*, ser. Physiology of the joints : Annotated diagrams of the mechanics of the human joints / I.A. Kapandji. L.H. Honoré Übers. Churchill Livingstone, 1982.